

Surface Morphological Changes in Monolayers of Aromatic Polyamides Containing Various N-Alkyl Side Chains

Atsuhiro Fujimori,* Satoshi Chiba, and Natsuki Sato

Graduate School of Science and Engineering, Yamagata University, Jonan 4-3-16, Yonezawa, Yamagata, 992-8510, Japan

Yoko Abe and Yuji Shibasaki

Department of Chemistry and Bioengineering, Iwate University, 4-3-5 Ueda, Morioka, Iwate, 020-8551, Japan

Received: September 30, 2009; Revised Manuscript Received: January 4, 2010

We synthesized new aromatic polyamides (poly-(N-alkylated benzamides), abbrev. PABA_n) having both a rigid main chain and a flexible side chain with different lengths. We investigated the solid-state structures, that is, the molecular orientation and surface morphology, of organized molecular films of PABA_n by performing surface pressure-area (π -A) isotherm, in-plane and out-of-plane X-ray diffraction (XRD), polarized infrared spectroscopy, and atomic force microscopy (AFM) measurements. The solid-state structure of poly-(N-methyl benzamide) (PABA₁) belonged to the monoclinic system, whereas PABA₃, PABA₄, and PABA₅ showed an orthorhombic packing pattern. PABA₇ and PABA₈ formed amorphous polymers. In the case of PABA₁₇, a two-dimensional hexagonal lattice was formed as a subcell consisting of side chains. These polymer monolayers were highly condensed on a water surface at 15 °C. Out-of-plane XRD measurement results showed that the PABA₁, PABA₃, PABA₄, and PABA₅ multilayers showed large periodicities of 50–60 Å. From AFM observation results, it was found that these aromatic polyamides formed single particle layers of hydrophilic groups localized at the bottom of the particles. On the other hand, PABA₇ and PABA₈ monolayers showed irregularity and exhibited shapeless morphologies. In addition, an organized molecular film of PABA₁₇ formed a highly ordered layer structure (periodicity of 30 Å) and a giant circular domain (diameter of 20 nm) made of a side chain crystal. The PABA₁₇ monolayer showed a hexagonal packing pattern formed due to van der Waals interaction between the flexible side chains. From these experimental findings, it was concluded that the polymer synthesis method employed in the present study can be directly used to control the crystal structure (the third order structure of polymers), molecular arrangement, and surface morphologies of polymer monolayers.

1. Introduction

Functional polymers, which are precisely controlled molecular arrangements, and their organized molecular films¹ can be developed as potential candidates for fabricating biomimetic models² and molecular electronic devices,^{3–5} which have attracted considerable interest in fundamental science; further, these molecular assemblies have several other potential applications.⁶

It is commonly known that crystalline polymers can be used to form hierarchical structures ranging in size from nanometer-scale lamellae to mesoscopic-scale spherulites.^{7–9} These crystalline polymers are generally formed by the folding of the main chain. Side chain crystalline comb polymers show two types of structural characteristics. It is known that comb polymers, which have crystallizable long n-alkyl side chains attached to an amorphous main chain, are packed into a layer structure along the *c*-axis and a subcell consisting of the side chains in the *ab*-plane.^{10,11} This subcell structure¹² is formed as a two-dimensional lattice, and the layer structure along the *c*-axis often reflects the large spacing between the main chains in the accumulated double layer structures. Octadecyl-based materials, which are types of long-chain compounds and are cocrystallized

with another hydrocarbon to incorporate the hydrocarbon into the same crystalline lattice, have found numerous industrial applications such as pour point depressants for lubricating oils or fuels, rheological modifiers, additives for petroleum products, and smart gels.¹³

Platé and Shibaev¹⁴ have studied these comb polymers extensively. An X-ray diffraction profile of the comb polymers showed an intense reflection corresponding to a Bragg spacing *d* of 4.2 Å, which suggested the formation of a hexagonal crystalline lattice of n-alkyl side chains. Further, reflection occurred in small-angle regions, which was considered to originate from the layer structure. The periodicity of the crystalline–amorphous layer can be obtained by estimating the diffraction angle of this reflection.

Indeed, these comb polymers are essentially attractive materials in the scientific field because of the difference in the solid-state nature between main chains and side chains. These polymers generally afford long-range phase segregated structures.^{15,16} Comb polymers consisting of a crystalline main chain attached to an amorphous side chain¹⁷ and an amorphous main chain attached to a crystalline side chain¹⁸ have been extensively studied and well reviewed in terms of their chemical¹⁹ and physical properties.²⁰ The movement of the crystalline segment is more or less inhibited by the amorphous segment; thus, various segregated structures are formed from similar materials.

* To whom correspondence should be addressed. Tel and Fax: +81-238-26-3073. E-mail: fujimori@yz.yzmzgata-u.ac.jp.

Much attention has been focused on crystalline–crystalline comb polymers,²¹ especially aromatic main chain polymers,²² because the packing geometry of bulky aromatic main chain polymers can vary due to the difference in the crystallinity of the side chains. Kevlar, poly(*p*-phenylene terephthalamide) (PPTA), was first functionalized using linear hydrocarbons having chain lengths of 3, 4, 7, 12, and 18 carbon atoms by means of the metalation of PPTA using sodium hydride (degree of substitution (DS) of 86–99%, inherent viscosity (η_{inh}) of 0.06–0.14), and the packing mode was investigated; the resulting comb polymers except that with the C₁₈H₃₇ side chain were all amorphous.²³ Poly(3-*n*-alkyl-4-oxybenzoate)s (PAOBA)s with alkyl side chain lengths varying from 1 to 18 carbon atoms were prepared, and their phase properties were fully investigated.²⁴ Poly(*N*-alkyl-*p*-benzamide) (PABA_n, DS > 96%) (10–18 carbon atoms) was prepared by the metalation method as well, and its packing structure was investigated.²⁵

The characteristics and properties of solid-state structures are closely related to the ability of these polyamides to form organized molecular films.^{26,27} Almost all side chain crystalline comb polymers have hydrophilic groups in the main chain, corresponding to amphiphiles, and these polymers can form a monolayer on a water surface. Further, such amphiphilic polymers are generally easy to transfer and they tend to pile up on a solid substrate. They form a highly ordered layer structure of multilayer films. Kunitake et al. characterized a polyelectrolyte-protein multilayer film by several microscopy and IR spectra techniques.²⁸ Du et al. analyzed the molecular orientation of LB multilayers of *N*-octadecyl-L-alanine formed on a water surface by IR and IR-RAS spectroscopy.²⁹ Itoh et al. determined the dichroic ratios of LB films of several amino acid derivatives and carried out their structural analysis by IR spectroscopy.³⁰ Lahav and Leiserowitz conducted pioneering studies on the wettability measurement of Z-type LB multilayers of alkyl gluconamides.³¹ Regen et al. carried out a study on the structural control of LB films of calyx[6]arene containing amino groups.³² Further, Myles et al. formed a mixed self-assembled monolayer containing bis(2, 6-diaminopyridine)amide on gold.³³ Meijer et al. investigated the energy transfer mechanism of LB films of dendrimers containing an amino group.³⁴ Oliver et al. studied the kinetics of the formation of an amino bond at the air/water interface by NMR spectroscopy.³⁵ Recently, Amabilino et al. fabricated supramolecular conduction nanowires with an amino bond.³⁶

In our previous study, we mainly reported the side chain packing of hydrogenated and fluorinated comb copolymers with different lengths in bulk and organized molecular films.³⁷ These fluorinated comb polymers formed an extremely stable monolayer on a water surface. This film was then transferred onto a solid surface, and it formed a phase-separated structure with a thickness of the order of several nanometers. Hydrogenated domains with diameters of the order of 10–20 nm were observed in this phase-separated surface structure of monolayers.

In the present study, new aromatic polyamides with a rigid main chain and flexible side chain having different lengths (poly(*N*-alkylated benzamide), abbrev. PABA_n, Figure 1) were synthesized. The solid-state structures, that is, the molecular orientation and surface morphology, of organized molecular films of these polymers were investigated by performing surface pressure–area (π -A) isotherm, in-plane and out-of plane X-ray diffraction (XRD), polarized infrared (IR) spectroscopy, and atomic force microscopy (AFM) measurements. It was possible to control the molecular arrangement and morphologies of these systematic polymer samples by preparing organized molecular

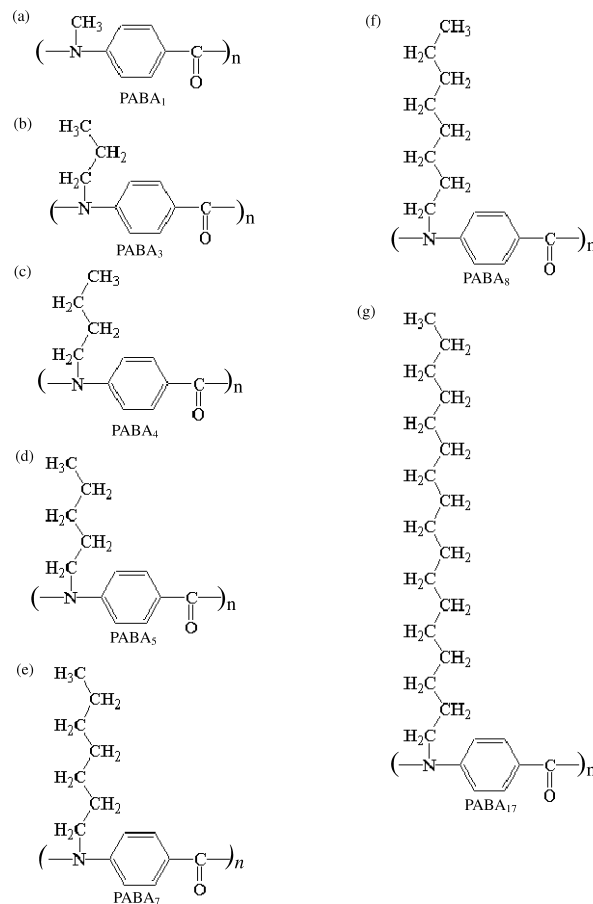


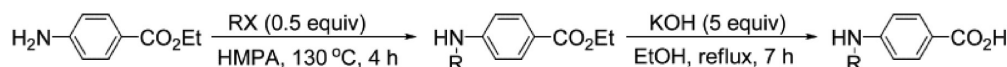
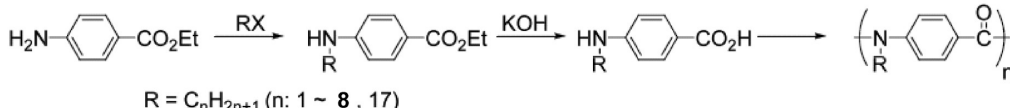
Figure 1. Chemical structure of aromatic polyamides with various side chains. (a) Methyl, (b) propyl, (c) butyl, (d) pentyl, (e) heptyl, (f) octyl, and (g) stearyl substituents.

films. Further, we have discussed the possibility of using these polyamides as new polymer nanomaterials.

2. Experimental Section

2.1. Materials.³⁸ **2.1.1. Synthesis of Monomer.** 4-Aminobenzoic acid ethyl ester and 4-(*N*-methyl)aminobenzoic acid were purchased from Wako Pure Chemical Co. Ltd. and used as received. Dry pyridine was purchased from Kanto Chemical Co. Inc. and used under nitrogen atmosphere. Hexamethyl phosphoramide (HMPA) was dried over calcium hydride and distilled under reduced pressure. Other reagents and solvents were used as received.

4-(*N*-propyl)aminobenzoic acid was poured into a three-necked flask equipped with a reflux condenser, thermometer, and three-way stopcock. 4-Aminobenzoic acid ethyl ester (79.3 g, 0.480 mol) was then added to this flask under nitrogen atmosphere. HMPA (222 mL) was added to this flask, and the mixture was stirred at 20 °C until the solid was completely dissolved. 1-Iodopropane (42.9 g, 0.252 mol) was then added to this solution, and the mixture was stirred at 130 °C for 4 h. The resultant mixture was poured into water (1 L), and the precipitate was washed with a methanol/water (1:5 in volume) mixed solvent to remove the residual solvent and salt. The solid was collected by filtration, purified by recrystallization from methanol, and dried at 80 °C for 12 h to give ethyl-4-(*N*-propyl)aminobenzoate. Ethyl-4-(*N*-propyl)aminobenzoate (38.3 g, 0.185 mol) thus obtained was placed in a 500 mL two-necked flask equipped with a reflux condenser. Potassium hydroxide (56.8 g, 0.923 mol) and ethanol (450 mL) were added to this

SCHEME 1: Monomer Synthesis Procedure and Polymerization Reaction of Aromatic Polyamides**Monomer Synthesis****Direct polycondensation**

flask and heated to 90 °C. After 7 h, the reaction mixture was poured into water, and the pH of the solution was adjusted to be around 4 by adding hydrogen chloride solution. The precipitate was collected, washed with water, recrystallized with methanol, and dried at 80 °C for 12 h to give the title compound. The other 4-(N-alkyl)aminobenzoic acid compounds were prepared in a similar manner as described above.

2.1.2. Direct Polycondensation of PABA_n. PABA_n compounds used in this study were synthesized by the direct condensation polymerization of *N*-alkylated aminobenzoic acid with methyl, propyl, butyl, pentyl, heptyl, octyl, and stearyl substituents (Scheme 1). PABA₁ was prepared and poured into a three-necked flask equipped with a reflux condenser, three-way stopcock, and thermometer. *N*-Methylaminobenzoic acid (4.55 g, 30.1 mol), triphenylphosphine (9.44 g, 36.0 mmol), and pyridine (30 mL) were then added to the flask. The mixture was stirred until the solid was dissolved. Hexachloroethane (8.52 g, 36.0 mmol) was then added to this solution, and the mixture was refluxed for 24 h. After the solution was cooled to room temperature, methanol/hydrogen chloride was added and stirred for 5 h. The precipitate was collected, washed with hot water, and dried at 220 °C for 24 h to give the PABA₁ compound. The other PABA_n compounds were prepared by the same method, as described above. The average molecular weights, M_w, of these aromatic polyamides were 20 000–90 000.

2.2. Structural Estimation in Bulk. Methods of structural estimation are shown as Supporting Information.

2.3. Formation of Polymer Monolayers on Water Surface and Observation of Molecular Arrangement in the Films. Monolayers of aromatic polyamides prepared from *m*-cresol or chloroform or trifluoroacetic acid solutions (about 10⁻⁴ M) were formed on distilled water (about 18 MΩcm). The surface pressure–area (π -A) isotherms of the polyamide monolayers were measured on a film balance (Kyowa Kaimen Kagaku Co. Ltd., compression speed: 3 cm/min) at 15 °C. These aromatic polyamides formed highly condensed monolayers. These monolayers were transferred onto solid (glass) substrates at 15 °C, and an appropriate surface pressure (15–25 mN m⁻¹) was applied to obtain alternating Y-type films by the Langmuir–Blodgett (LB) method.^{1,39,40} Hydrophobic side chains on the outermost surface of Z-type LB films transferred onto solid substrates were exposed to air.

Methods of estimation of molecular arrangement and observation of surface morphology in the two-dimensional films are shown as Supporting Information 1.

3. Results and Discussion

3.1. Observation of Fine Structures of Bulky Aromatic Polyamides. Figure 2 shows wide-angle X-ray diffraction (WAXD) patterns and profiles of the bulky aromatic polyamides

with various side chains lengths, and Table 1 shows the *d*-spacing values obtained from the corresponding WAXD profiles. All the polymers except PABA₇ and PABA₈ show several sharp diffraction peaks, indicating crystalline structures. The WAXD profile of PABA₁ shows two clear peaks at 14.9 and 16.8° along with smaller ones at 8.4, 23.8, 25.8, and 29.2°. Characteristic well-developed peaks are observed at about 13 Å (2θ = 6.8°) in the profiles of PABA₃, PABA₄, and PABA₅. Such large spacing almost agrees with the periodic structure observed along the *c*-axis; however, crystalline polymers generally do not form such long periodic structures. This type of structure is often observed in crystalline polymers with helical conformation.^{41,42} The profiles of PABA₇ and PABA₈ show two types of halos, indicating the formation of amorphous structures. The PABA₁₇ monolayer having a longer alkyl side chain shows sharp peaks at 2θ = 2.9, 5.8, and 21.3° ($d_{001} = 30.5$ Å, $d_{002} = 15.2$ Å, and $d_{100} = 4.2$ Å, respectively), from which the side chain crystalline structure of PABA₁₇ is determined to correspond to a hexagonal packing structure. This structure is similar to that observed in conventional comb polymers.^{10,14,37}

To confirm the formation of more highly ordered structures in bulky poly-(*N*-alkylated benzamide), SAXS measurements were carried out. Figure S1 in Supporting Information shows SAXS patterns and profiles of bulky aromatic polyamides with methyl (PABA₁), propyl (PABA₃), butyl (PABA₄), pentyl (PABA₅), heptyl (PABA₇), and stearyl (PABA₁₇) substituents. At scattering angles below 2θ = 5° ($q = 3.5$ nm⁻¹), except in the case of PABA₁₇, additional scattering peaks corresponding to a more highly ordered structure are not observed. This result indicates that these aromatic polyamides cannot form a lamellar structure by the folding of the polymer main chain, because the absence of peaks corresponding to crystalline polymers implies the lack of a lamellar interface. On the other hand, PABA₁₇ exhibits two types of scattering peaks at the same position in the WAXD pattern. These peaks can be attributed to the formation of head-to-head and tail-to-tail double layer structures along the *c*-axis.

Figure 3 shows a schematic illustration of packing models with a reciprocal lattice of bulky aromatic polyamides with methyl groups (PABA₁), propyl to pentyl groups (PABA_{3–5}), and stearyl groups (PABA₁₇) as the side chain. The WAXD patterns and corresponding peak positions on the reciprocal lattice suggest that PABA₁ shows a monoclinic lattice structure with order parameters of $\alpha = \gamma = 90^\circ$, $\beta = 67.5^\circ$, $a = 7.7$ Å, $b = 5.7$ Å, and $c = 10.8$ Å. On the other hand, PABA_n ($n = 3, 4$, and 5) show an orthorhombic lattice structure, again with $\alpha = \beta = \gamma = 90^\circ$, $a = 7.7$ Å, $b = 5.6$ Å, and $c = 13.0$ Å. The short methyl moiety of PABA₁ could distort the crystal lattice to afford a packing structure that is different from the others. In addition, the periodicity of 10.8 Å observed in the case of

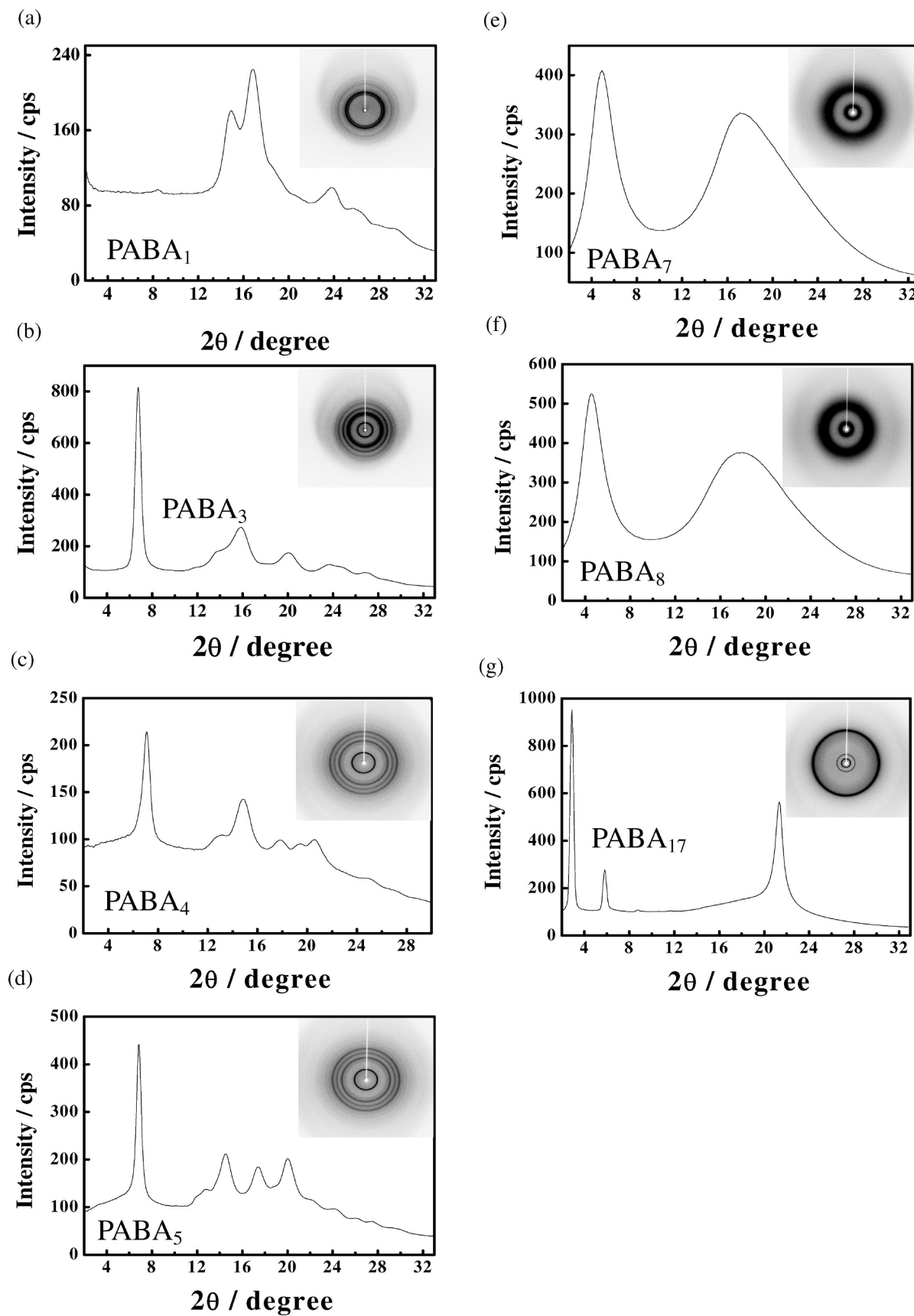


Figure 2. WAXD patterns and profiles of aromatic polyamides with various side chains in bulk. (a) Methyl, (b) propyl, (c) butyl, (d) pentyl, (e) heptyl, (f) octyl, and (g) stearyl substituents.

PABA₁ and 13.0 Å in the case of PABA_n ($n = 3, 4$, and 5) could be attributed to the pitch of the helix formed due to the structural propensities of the cis conformation of N-alkylated

amide bonds and syn arrangement of the benzene ring.⁴³ Several researchers have studied the crystalline structure of PABA₀ (polybenzamide) with no alkyl side chains, where the polymers

TABLE 1: *d*-Spacing Value of Aromatic Polyamides with Various Side Chains Estimated by WAXD in Bulk

2θ/degree		<i>d</i> (Å)
8.4 14.9 16.8 23.8 25.8 29.2	PABA ₁	10.5 5.9 5.3 3.7 3.5 3.1
	PABA ₃	13.0 6.5 5.6 4.4 3.4 3.3
	PABA ₄	12.5 5.9 5.3 3.7 3.5 3.1
	PABA ₅	12.8 7.0 6.1 5.1 3.7
	PABA ₇	18 5.2
	PABA ₈	19.2 5.0
	PABA ₁₇	30.5 15.2 4.2

are tightly packed to form orthorhombic systems due to the hydrogen bonding of amide groups (trans conformation) (order parameters of $a = 7.74$, $b = 5.27$, and $c = 12.82 \text{ \AA}$).⁴⁴ The WAXD profiles of PABA₇ and PABA₈ show disordered structures. According to the extended structure of polyethylene, an increase of CH_2 resulted in an increase of 1.25 \AA spacing.⁴⁵ Thus, the spacing of the double layer structure of the side chain crystal domain is calculated to be $1.25 \text{ \AA} \times 2 \times 17 = 42.5 \text{ \AA}$. The WAXD profile of PABA₁₇ shows a spacing of 30.5 \AA , which is much smaller than the calculated value. Therefore, the PABA₁₇ side chain shows a highly tilted orientation, as shown in Figure 3c.

In other words, the solid-state structure of N-alkylated polyamide films with various lengths depends on the side chain length. PABA_{1–5} form crystal structures packed with rigid main chains. PABA_{3–5} show orthorhombic packing, whereas only PABA₁ forms a distorted monoclinic structure. On the other hand, PABA_{7–8} do not form a crystal structure and are transformed into an amorphous structure. It is believed that the steric hindrance of longer side chains obstructs the formation of a crystal structure. The crystal structure of PABA₁₇, which has a long side chain, is not packed with rigid main chains. This compound shows hexagonal packing due to the van der Waals interaction between the flexible side chains. From these experimental findings, it is concluded that the polymer synthesis

method employed in this study can be directly used to control the crystalline morphology (the third order structure of polymers) of polymer monolayers.

A solid-state structural analysis, that is, the formation and structure, of two-dimensional organized molecular films of poly-(N-alkylated benzamides) is carried out.

3.2. Monolayer Behavior and Molecular Arrangement of Organized Molecular Films of Aromatic Polyamides. π -A isotherms of aromatic polyamide monolayers with methyl (PABA₁), propyl (PABA₃), butyl (PABA₄), pentyl (PABA₅), heptyl (PABA₇), octyl (PABA₈), and stearyl (PABA₁₇) substituents formed on the water surface at 15°C are shown in Figure 4. PABA₁ forms a stable condensed monolayer in a single condensed state. Further, the limiting area of this material indicated relatively smaller value (18 \AA^2) than the dominated area of hydrocarbon chains in general amphiphiles. In the case of PABA₃, PABA₄, PABA₅, and PABA₇ monolayers formed on the water surface, the presence of two condensed states and plateau regions is confirmed. However, the isotherms in both the low- and high-surface pressure regions indicate a tilted crystal orientation. From these isotherms, it is difficult to judge whether the plateau region corresponds to a two-dimensional phase transition or collapsed surface pressure. The aromatic polyamides used in this study essentially have weak hydrophilic groups. In addition, the isotherm of the PABA₈ monolayer does not indicate the formation of a second condensed layer. The above-mentioned findings indicate that it is very likely that a second condensed monolayer was not formed, and hence, the aromatic polyamides piled up on the water surface. Further, the isotherm of the PABA₁₇ monolayer having long hydrophobic chains shows a plateau region and two condensed states. These monolayers of aromatic polyamides were transferred at high surface pressure region after the plateau of isotherm, except for the PABA₈.

Out-of-plane XRD profiles of the first condensed layer of the poly-(N-alkylated benzamide) LB multilayers formed on the water surface are shown in Figure 5. Quite interestingly, all the polymers except PABA₇ and PABA₈ show a layer spacing of around $50–60 \text{ \AA}$ along the *c*-axis. Only the PABA₁₇ LB film shows almost the same large spacing as that in the bulk state. The LB films of PABA_{1–8} show very large spacing. On the other hand, in-plane XRD measurements indicate that these LB films show irregularity in the film plane (Figure 6). Only the PABA₁₇ multilayer shows a two-dimensional lattice spacing of 4.2 \AA due to the formation of a subcell structure made of the stearyl side chain. All the other polyamide LB multilayers form an amorphous structure in the *ab*-plane. The PABA₁, PABA₃, PABA₄, and PABA₅, which become a crystal at the bulk state, form amorphous nanoparticles at the air–water interface. In the bulk state, these aromatic polyamides do not form lamellae crystal made by folded polymer main chain. These polymers form the extended chain crystal (ECC) based on the SAXS results, which do not show the existence of lamellae interface in polymer solids. At the air–water interface, the main chain itself of aromatic polyamides in the films are piled up along the height direction and form the nanoparticles because contact area of less hydrophilic aromatic polyamide chain to the water surface become small. Since the piled up molecular-chains cannot form the microscopic regularity, these nanoparticles may be become amorphous structure. In general, amorphous polymer LB films with a nanometer-order stable layered structure are highly durable.^{46–48} These aromatic polyamide LB films can be used to fabricate new nanomaterials because of their amorphous layered structure.

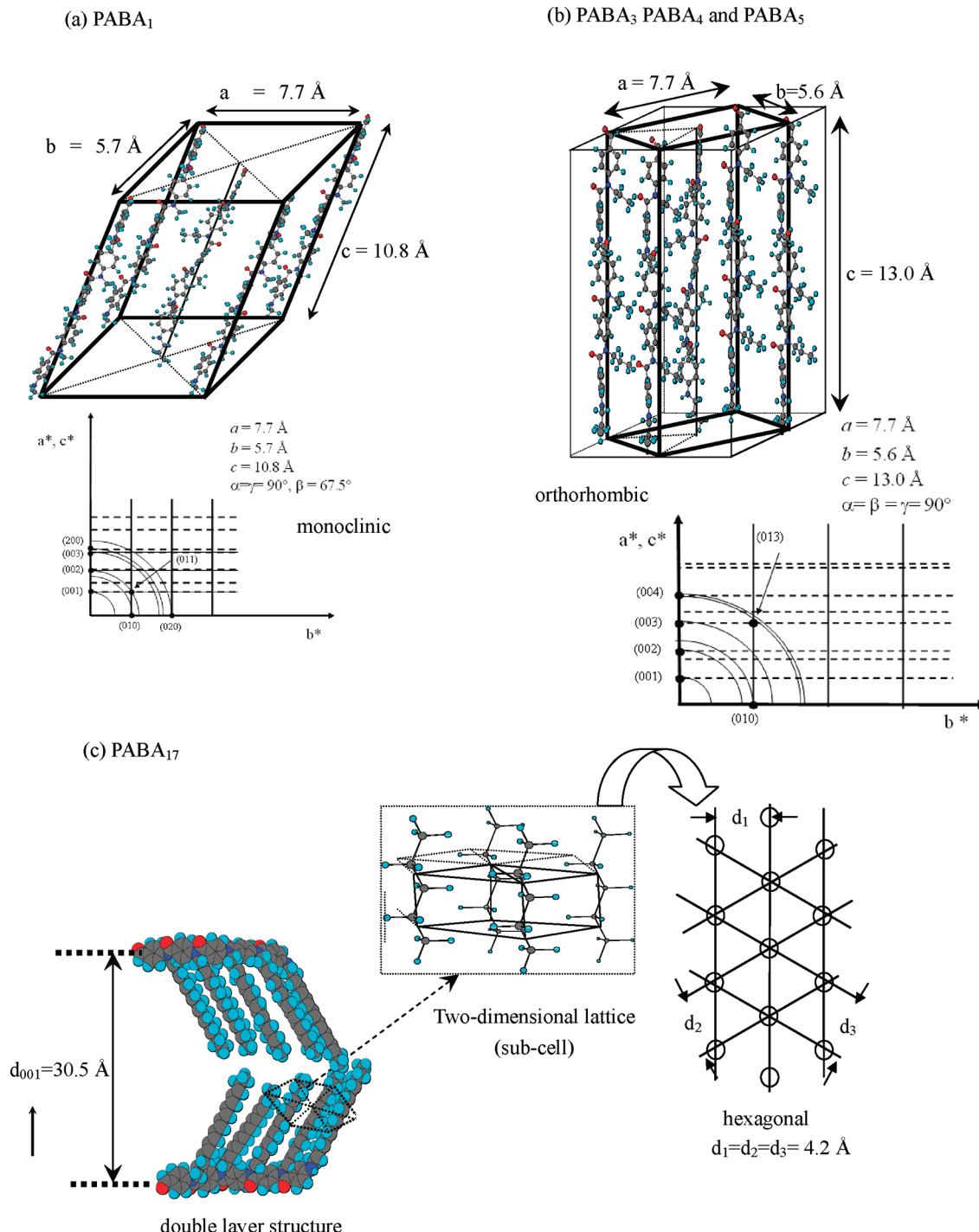


Figure 3. Schematic illustration of packing models with reciprocal lattice of (a) aromatic polyamides with methyl groups as the side chain, (b) propyl, butyl, and pentyl groups as the side chain, and (c) stearyl groups as the side chain in bulk.

Figure S2 in Supporting Information shows transmission IR spectra of aromatic polyamide LB multilayers transferred onto a CaF₂ substrate. C—H symmetric and asymmetric stretching vibration bands observed around 2800–3000 cm⁻¹ gradually increase in size with the side chain length of the poly-(N-alkylated) polyamides. Further, carbonyl bands in the amide group and C=C stretching vibration bands of phenyl groups are clearly observed at 1650 and 1600 cm⁻¹ in the spectra. To qualitatively investigate the molecular arrangement in the LB films, these two types of IR bands are studied and polarized IR measurements are carried out (Figure 7). These two bands are deconvoluted by Gaussian fitting, and values of individual peak areas are utilized by equation of dichroic ratio applied to uniaxial

orientation. As a result, carbonyl bands in both amide and phenyl groups in the PABA₇ LB film, which does not form a layer structure along the c -axis but forms an amorphous structure in the film plane, are not oriented. Although the PABA₁ and PABA₄ LB films show irregularity in phenyl groups, other functional groups in the polyamide LB films exhibit an orientation angle of around 40–50°. In other words, it is found that almost all the functional groups in the main chains show highly tilted orientation in the film.

As mentioned above, the molecular orientation, crystallinity, and regularity of organized molecular films of poly-(N-alkylated) polyamides are studied by performing two types of X-ray diffraction and polarized IR spectroscopy measure-

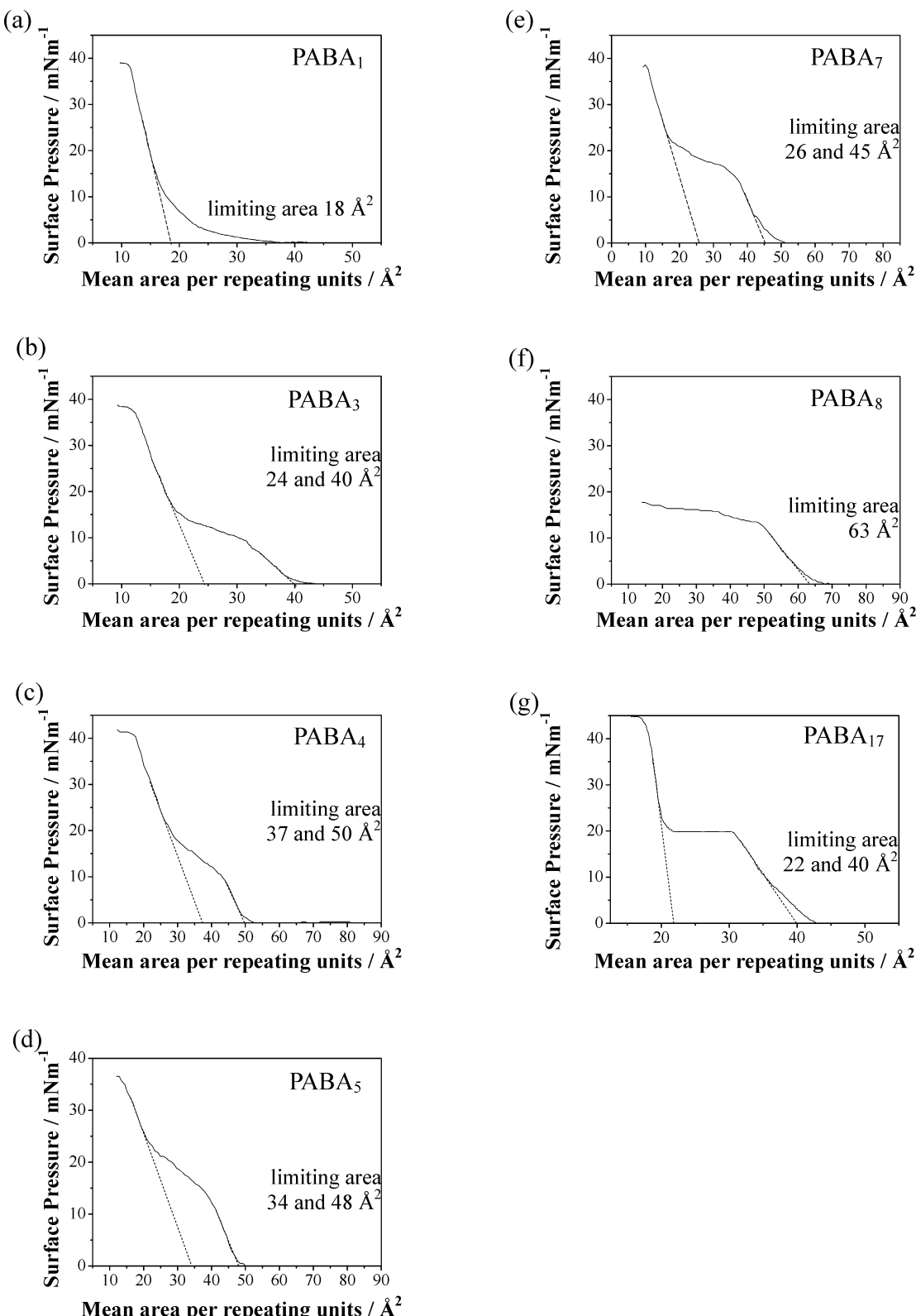


Figure 4. Surface pressure-area isotherms of monolayers on the water surface of aromatic polyamides with various side chains in bulk. (a) Methyl, (b) propyl, (c) butyl, (d) pentyl, (e) heptyl, (f) octyl, and (g) stearyl substituents at 15 °C.

ments. In the next section, the relationship between the surface morphology and molecular arrangement is mainly discussed.

3.3. Side Chain Length Dependency of Surface Morphology of Aromatic Polyamide Monolayers. Figure 8 shows AFM images of Z-type aromatic polyamide monolayers transferred onto a mica substrate. Observations suggest that the PABA₁,

PABA₃, PABA₄, and PABA₅ films are a single particle layer having a height of 26–36 Å. The twice value of particle height are almost same to the long spacings estimated by out-of-plane XRD. Indeed, average transfer ratio of monolayers of PABA₁, PABA₃, PABA₄, and PABA₅ is 1.4 (over 1.0) whereas that of PABA₁₇ monolayer exhibits almost 1.0. The length of polymer main chain inferred from molecular weight ($M_w = 20\,000$ –90 000)

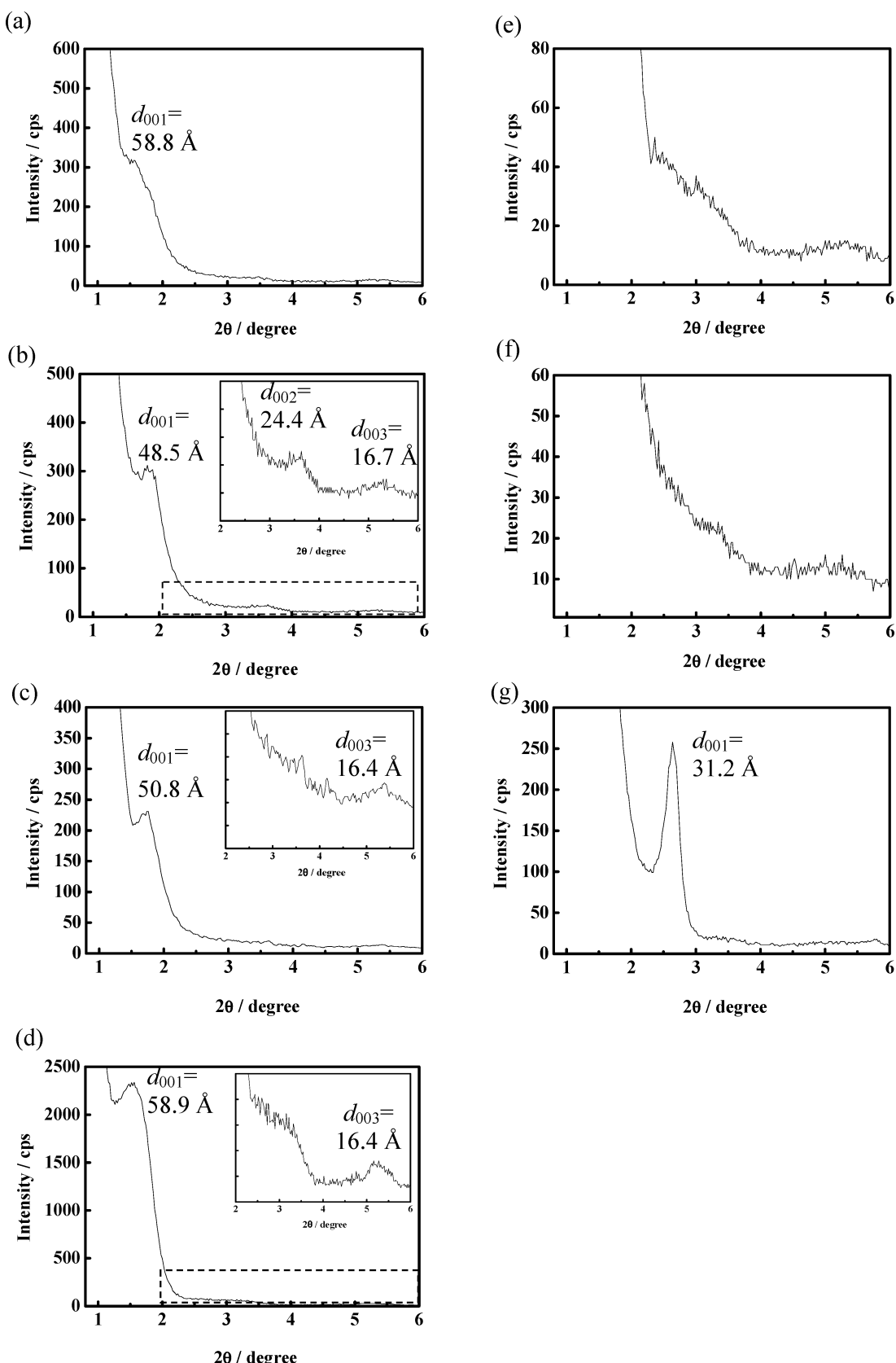


Figure 5. Out-of plane XRD profiles of LB multilayers (20 layers) of aromatic polyamides with various side chains. (a) Methyl, (b) propyl, (c) butyl, (d) pentyl, (e) heptyl, (f) octyl, and (g) stearyl substituents.

exhibits the range from 25 to 75 nm. Height of formed nanoparticles is 26–36 Å. In the case of length of polymer main chain of 50 nm and thickness of a polymer-chain of 0.5 nm (calculated by a simple molecular modeling), polymer main

chain fold at 5–6 times and the length of this folded unit indicates the 8–10 nm to exhibit 26–36 Å height of nanoparticles. Generally, it is well-known that lamellae thickness of crystalline polymer converges to about 10 nm size.^{7–9} This

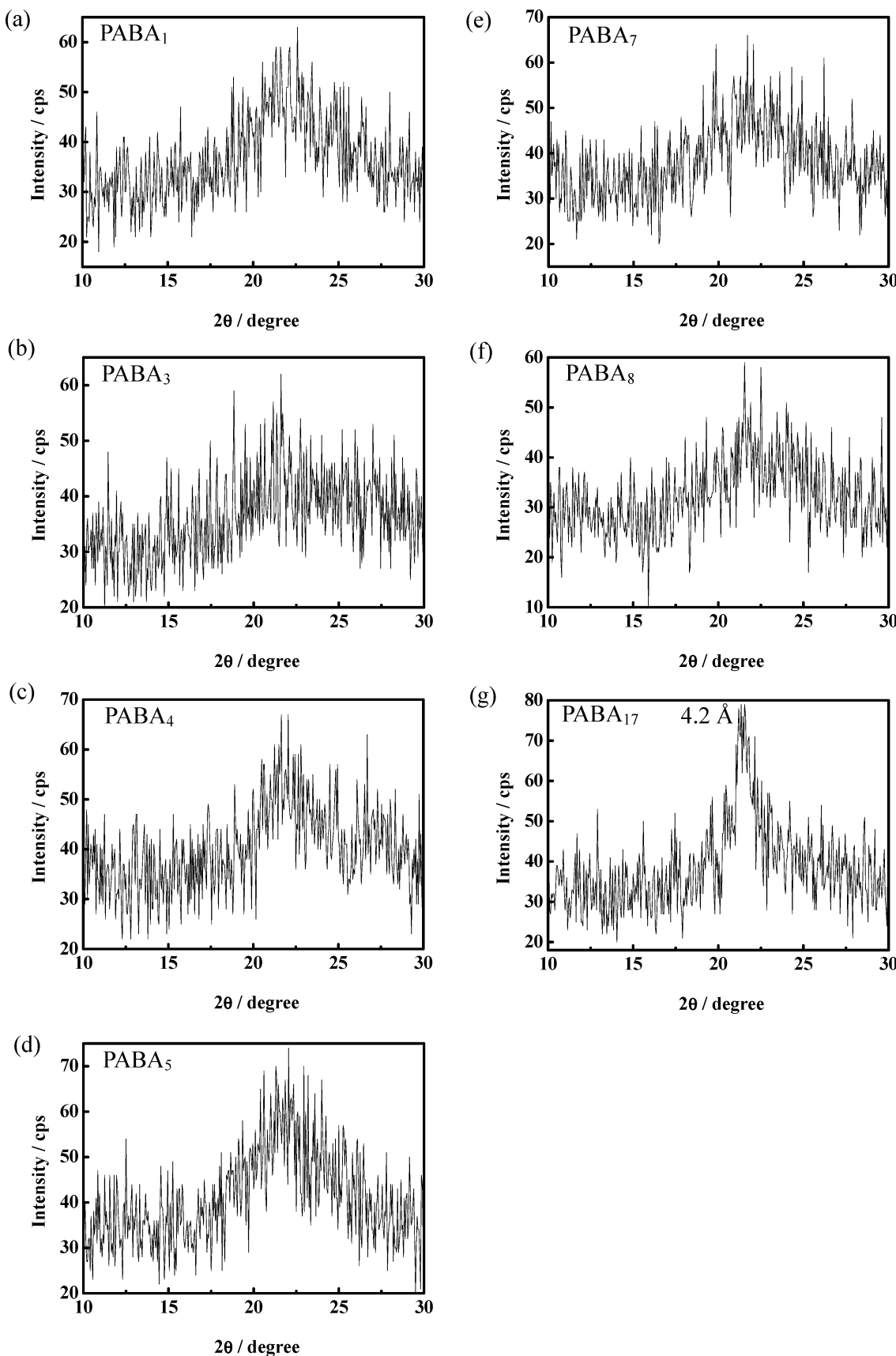


Figure 6. In-plane XRD profiles of LB multilayers (20 layers) of aromatic polyamides with various side chains. (a) Methyl, (b) propyl, (c) butyl, (d) pentyl, (e) heptyl, (f) octyl, and (g) stearly substituent.

analogy may suggest a dependency on molecular weight related to the size of nanoparticles. The origin of small dispersion of particle height in this study may be based on the use of relative

low-molecular weight polymers. The PABA₇ and PABA₈ monolayers show shapeless domains. In the case of the PABA₁₇ monolayer, the formation of giant circular domains with a

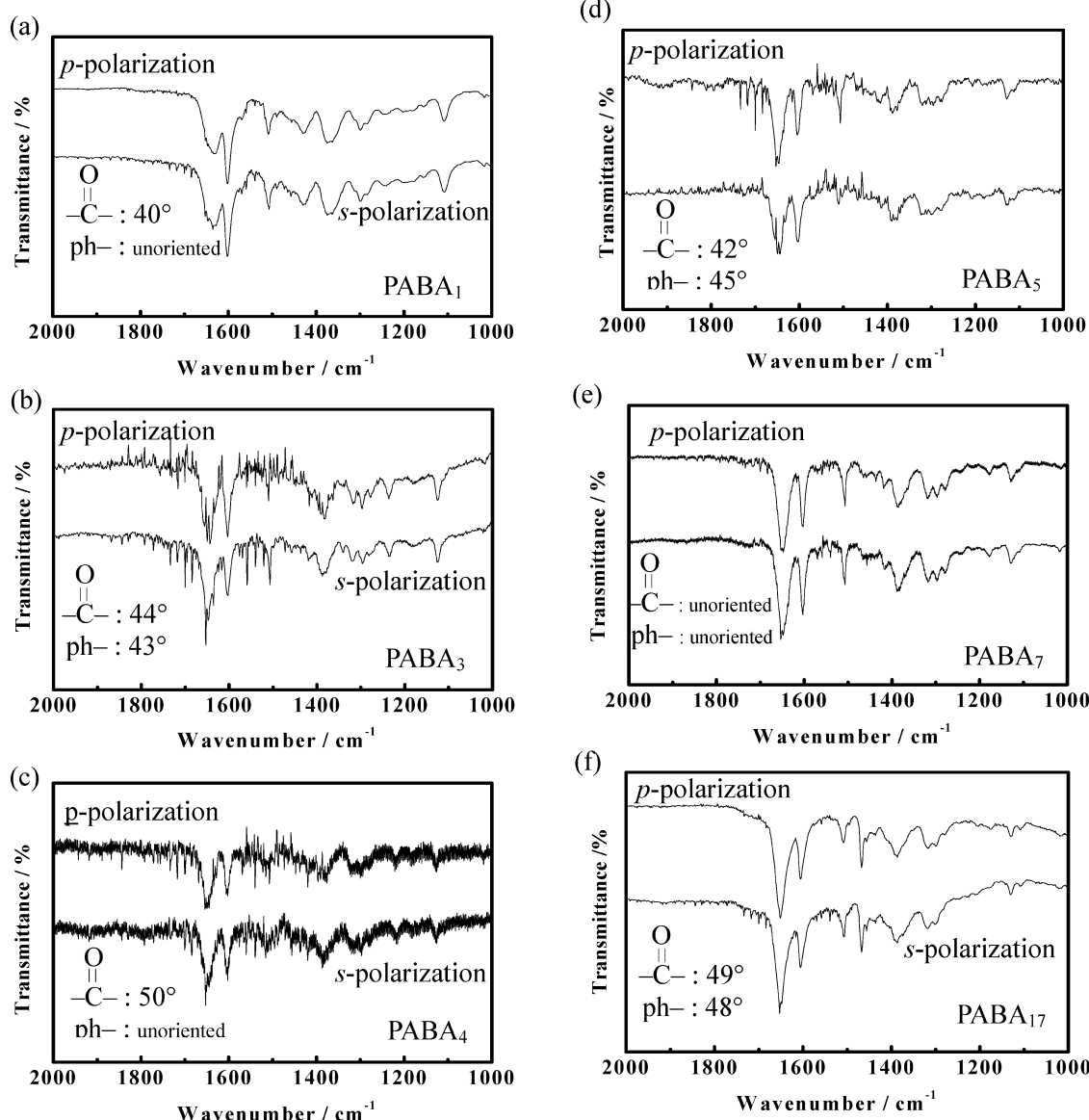


Figure 7. Polarized IR spectra of LB multilayers (20 layers) of aromatic polyamides with various side chains. (a) Methyl, (b) propyl, (c) butyl, (d) pentyl, (e) heptyl, and (f) stearyl substituents on CaF₂ substrate. (Inset) Estimated orientation angle of carbonyl groups and phenyl groups.

diameter of 20 nm is observed. Moreover, the surface of this domain is flat on a mesoscopic level.

Figure 9 shows highly magnified AFM images of Z-type PABA₅, PABA₇, and PABA₁₇ monolayers transferred onto a mica substrate. In the case of the PABA₅ single particle layer, polyamide particles are widely distributed over a probing area of 5 × 5 μm². Since the average height of these particles is 2.8 nm, periodic structure of double particle layers is corresponding to the results of out-of-plane XRD. Hydrophilic groups such as carbonyl groups are formed in these polymer particles at the air/water interface, and these groups are assumed to localize at bottoms of particles. Therefore, these particles do not have a completely homogeneous structure, and it is considered that the spacing between the localized hydrophilic regions in the double particle layer can be estimated by performing out-of-plane XRD measurements. In mesoscopic-scale images of the PABA₇ monolayer, the presence of a sinewy domain is confirmed. According to the in-plane and out-of-plane XRD and polarized IR spectroscopy measurement results, the molecular arrangement in these shapeless domains is almost random. PABA₁₇ molecules are closely packed, and they form a side chain hexagonal lattice

in a giant flat domain of monolayer surface. This hypothesis is supported by both the in-plane and out-of-plane XRD measurement and AFM observation results. The polydispersity of the domain is significant in a large scan area of 50 × 50 μm². The PABA₁₇ monolayer is an assembly of circular domains of different sizes.

Figure 10 shows a schematic illustration of the aromatic polyamide films with methyl to pentyl groups (PABA_{1–5}), heptyl to octyl groups (PABA_{7–8}), and stearyl groups (PABA₁₇) as the side chain in the monolayers. The organized molecular films of PABA_{1–5} are found to be multiparticle layers, consisting of single particle polyamide layers. The hydrophilic groups in the individual particles are assumed to be localized at particle bottoms. The surface morphology of the PABA₇ and PABA₈ monolayers shows a shapeless sinewy domain. On the other hand, the PABA₁₇ monolayer forms a giant domain consisting of a closely packed hexagonal subcell.

As mentioned above, the crystal structure, two-dimensional molecular arrangement, and surface morphology of aromatic polyamide monolayers depend on the side chain lengths. In other words, the method used to form organized molecular films of

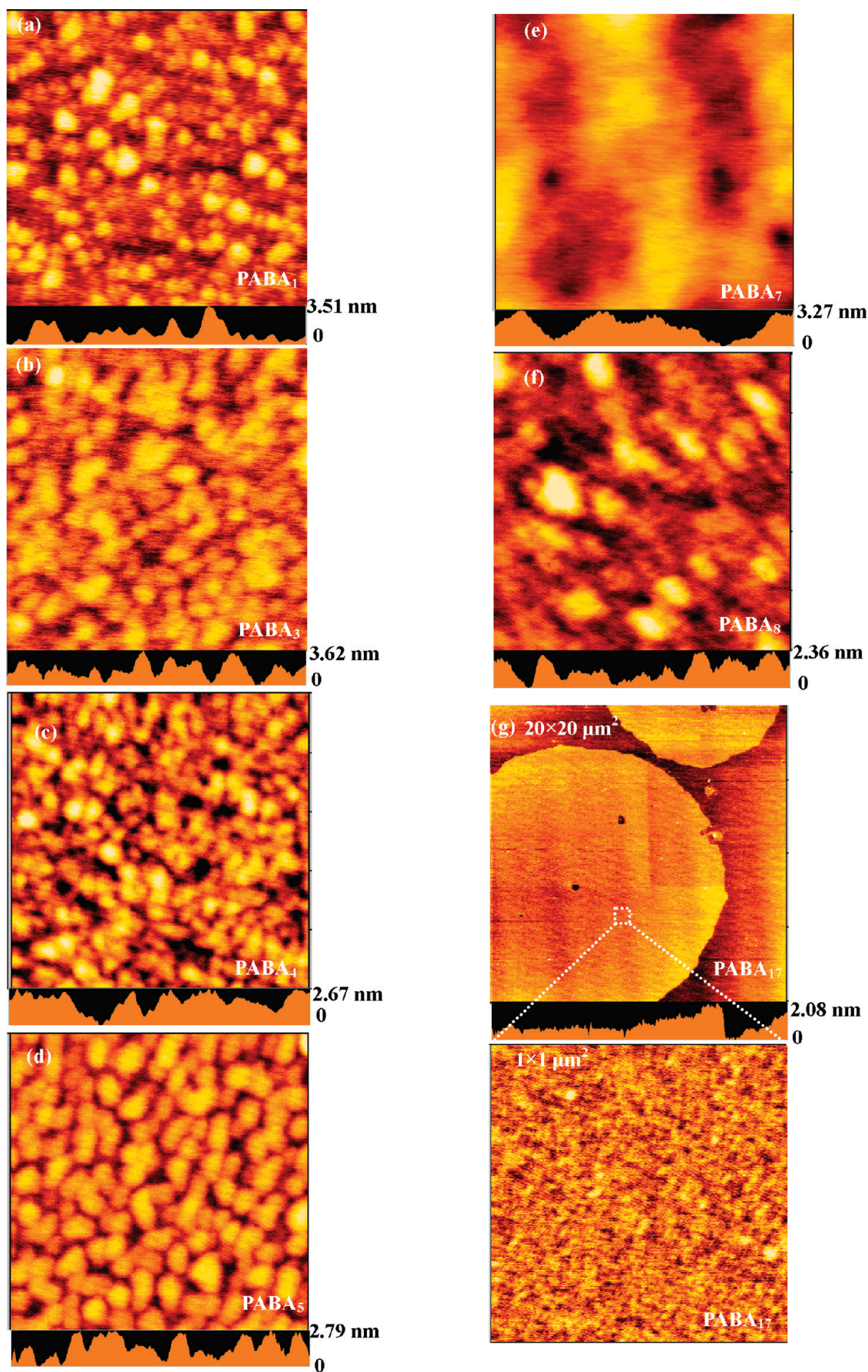


Figure 8. AFM images of Z-type monolayers on mica of aromatic polyamides with various side chains. (a) Methyl, (b) propyl, (c) butyl, (d) pentyl, (e) heptyl, (f) octyl, and (g) stearly substituents ($1 \times 1 \mu\text{m}^2$).

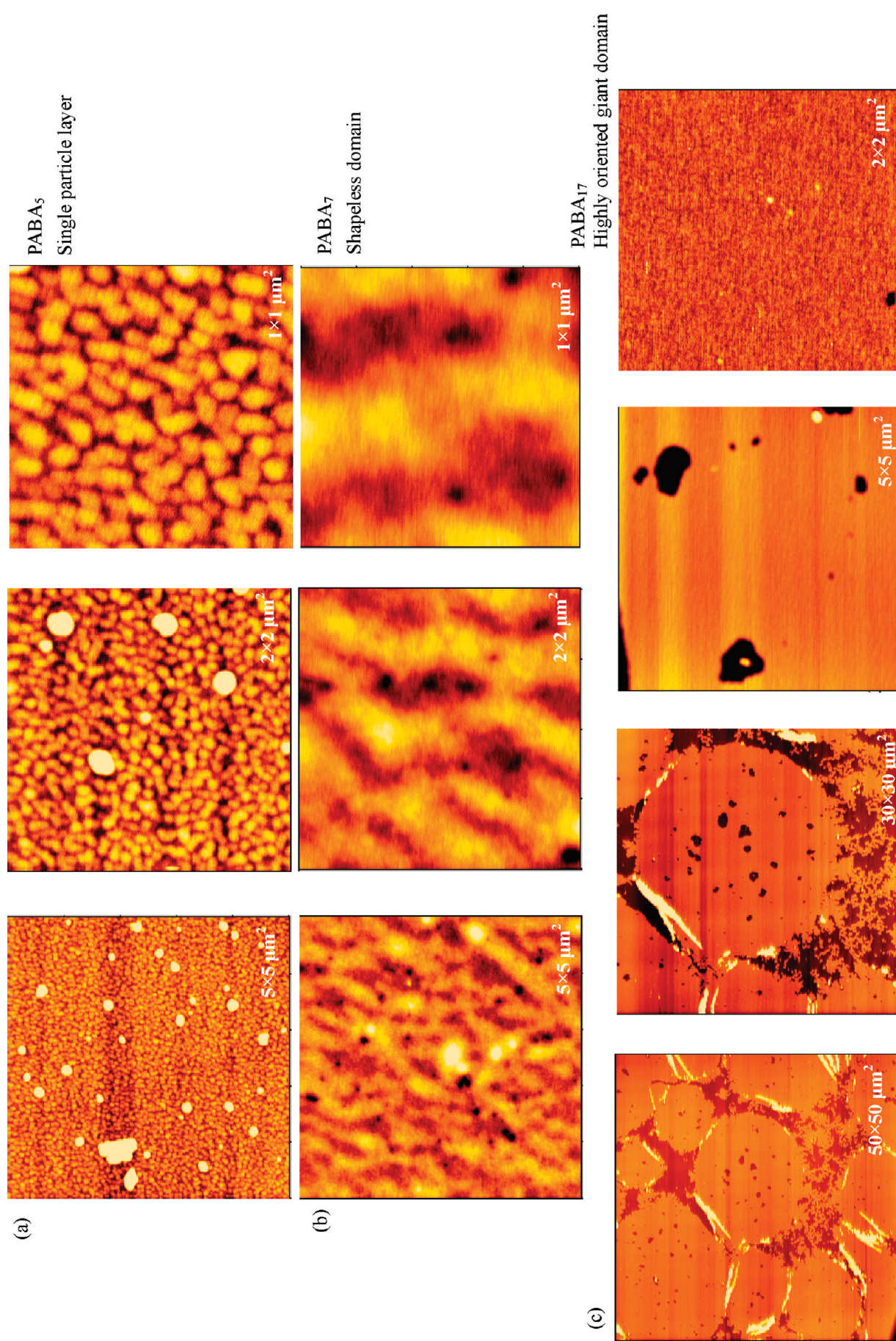


Figure 9. AFM images at several magnification of Z-type monolayers on mica of aromatic polyamides with (a) pentyl, (b) heptyl, and (c) stearyl side chains.

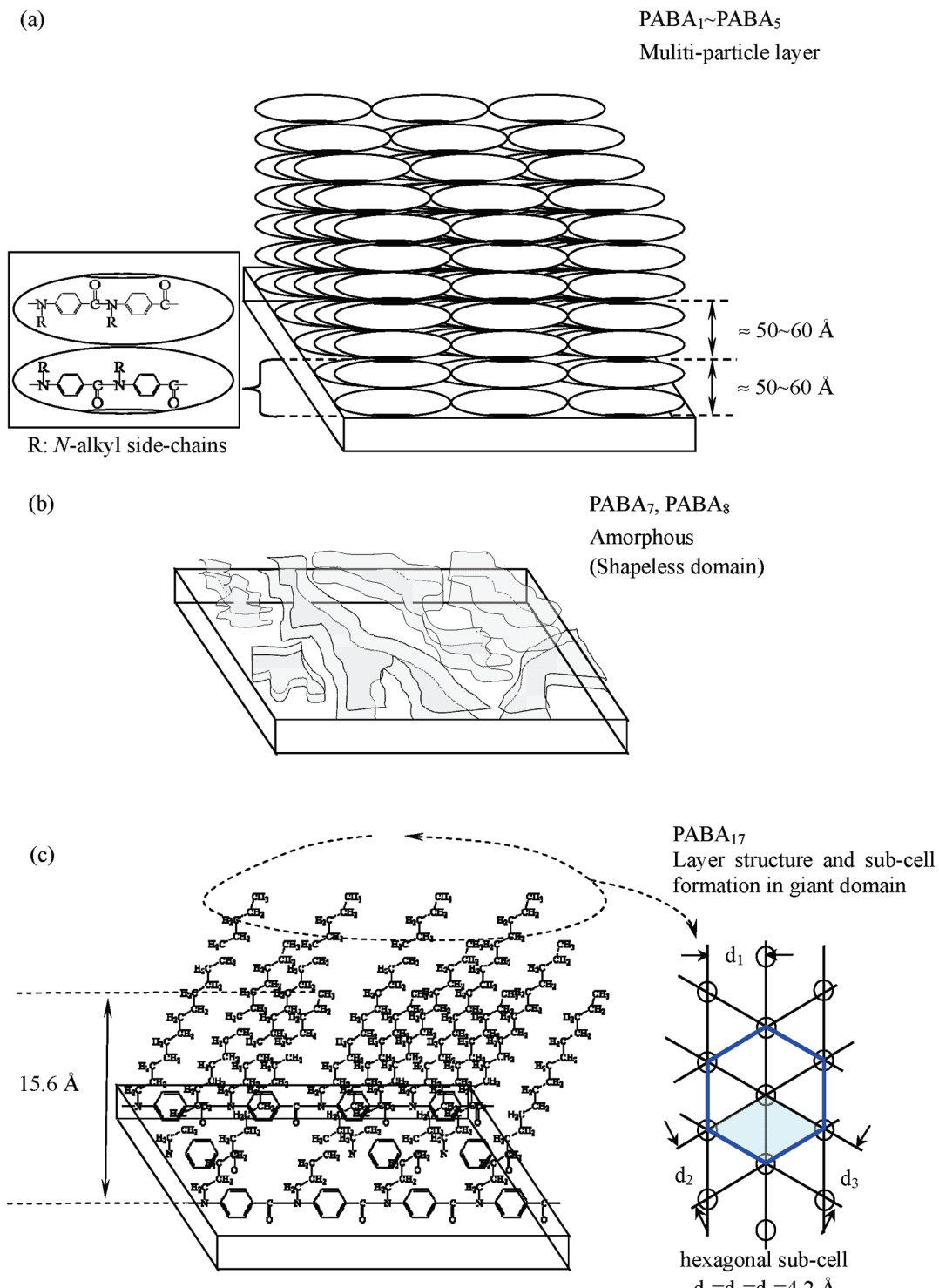


Figure 10. Schematic illustration of film structure (particle arrangement, mesoscopic morphology, or molecular packing) for aromatic polyamides with (a) pentyl, (b) heptyl, and (c) stearly side chains.

poly-(N-alkylated) polyamides in this study can be directly used to control the molecular packing and formation of characteristic morphologies from subnanometer scale to mesoscopic scale. We believe that this study is the first in which a detailed structural analysis, particularly both molecular arrangement and morphology, of organized molecular films of poly-(N-alkylated polybenzamides) with systematic side chains was carried out.

Conclusion

The solid-state structures, that is, the molecular arrangement and surface morphology, of organized molecular films of newly

synthesized aromatic polyamides with different lengths were investigated by performing π -A isotherm, in-plane and out-of-plane XRD, and polarized IR spectroscopy measurements and carrying out AFM observations. In the bulk state, only PABA₁ showed monoclinic packing, whereas PABA₃, PABA₄, and PABA₅ showed orthorhombic packing. On the other hand, PABA₇ and PABA₈ showed amorphous structures. PABA₁₇ formed a two-dimensional hexagonal lattice as a subcell made of side chains. The aromatic polyamide monolayers were highly condensed on the water surface at 15 °C. The layered structure of PABA₁, PABA₃, PABA₄, and PABA₅ multilayers showed

large spacings of 50–60 Å, as estimated from out-of-plane XRD measurement results. The AFM observation results suggested that these aromatic polyamides formed single particle layers, wherein hydrophilic groups localize at bottom of the particles. The PABA₇ and PABA₈ multilayers showed irregularity and exhibited shapeless morphologies. On the other hand, the organized molecular film of PABA₁₇ formed a highly ordered layer structure (periodicity of 30 Å), side chain crystal showing two-dimensional hexagonal packing, and giant domain (diameter of 20 nm). From these experimental findings, it is concluded that the polymer synthesis method employed in this study can be directly used to control the crystal structure, molecular arrangement, and surface morphologies of polymer monolayers.

Supporting Information Available: Description of Structural Estimation in Bulk and a part of Formation of Polymer Monolayers on Water Surface and Observation of Molecular Arrangement in the Films in Experimental Section. Figure S1. SAXS patterns and profiles of aromatic polyamides with various side chains in bulk (a) methyl, (b) propyl, (c) butyl, (d) pentyl, (e) heptyl, and (f) stearyl substituents. Figure S2. Transmission IR spectra of LB multilayers (20 layers) of aromatic polyamides with various side chains (a) methyl, (b) propyl, (c) butyl, (d) pentyl, (e) heptyl, (f) octyl, and (g) stearyl substituent on CaF₂ substrate. This material is available free of charge via the Internet at <http://pubs.acs.org>.

References and Notes

- (1) Gaines, G. L., Jr. *Insoluble Monolayers at Liquid Gas Interfaces*; Wiley: New York, 1966.
- (2) Kuhn, H., Möbius, D., Bucher, H. *Spectroscopy of Monolayer Assemblies*, in *Physical Methods of Chemistry*; Weissberger, A., Rossiter, B. W., Eds.; Wiley: New York, 1972; Vol. 1, Part IIIB, pp 577–702.
- (3) Roberts, G. G. *Langmuir-Blodgett Films*; Plenum Press: London, 1990.
- (4) Petty, M. C. *Langmuir-Blodgett Films*; Cambridge Univ. Press: New York, 1996.
- (5) Ulman, A. *Ultrathin Organic Films*; Academic Press: London, 1991.
- (6) Fukuda, K.; Shibasaki, Y.; Nakahara, H. *Thin Solid Films* **1983**, *99*, 87–94.
- (7) Keller, A. *Philos. Mag.* **1957**, *2*, 1171–1175.
- (8) Till, P. H. *J. Polym. Sci.* **1957**, *24*, 301–306.
- (9) Fischer, E. W. *Z. Naturforsch.* **1957**, *12a*, 753–754.
- (10) Inomata, K.; Sakamaki, Y.; Nose, T.; Sasaki, S. *Polym. J.* **1996**, *28*, 986–991.
- (11) Neugebauer, D.; Theis, M.; Pakula, T.; Wegner, G.; Matyjaszewski, K. *Macromolecules* **2006**, *39*, 584–593.
- (12) Vand, V.; Bell, I. P. *Acta Crystallogr.* **1951**, *4*, 465–469.
- (13) Baskar, G.; Ramya, S.; Mandal, A. B. *Colloid Polym. Sci.* **2002**, *280*, 886–891.
- (14) Shibaev, V. P.; Platé, N. A. *Adv. Polym. Sci.* **1984**, *60/61*, 173–260.
- (15) Riess, G.; Hurtrez, G.; Bahadur, P. In *Encyclopedia of Polymer Science and Engineering*; Mark, H. F., Kroschwitz, J. I., Eds.; Wiley: New York, 1985; Vol. 2, pp 324.
- (16) Hamley, I. W. *The Physics of Block Copolymers*; Oxford University Press: New York, 1998.
- (17) Watanabe, J.; Imai, K.; Gehani, R.; Uematsu, I. *J. Polym. Sci., Part B: Polym. Phys.* **1981**, *19*, 653–665.
- (18) Kaufman, H. S.; Sachen, A. *J. Am. Chem. Soc.* **1948**, *70*, 3147–3148.
- (19) Gao, H. F.; Matyjaszewski, K. *Prog. Polym. Sci.* **2009**, *34*, 317–350.
- (20) Peleshanko, S.; Tsukruk, V. V. *Prog. Polym. Sci.* **2008**, *33*, 523–580.
- (21) Harkness, B. R.; Watanabe, J. *Macromolecules* **1991**, *24*, 6759–6763.
- (22) Ballauff, M. *Angew. Chem., Int. Ed. Engl.* **1989**, *28*, 253–267.
- (23) Takayanagi, M.; Katayose, T. *J. Polym. Sci., A: Polym. Chem.* **1981**, *19*, 1133–1145.
- (24) Stern, R.; Ballauff, M.; Lieser, G.; Wegner, G. *Polymer* **1991**, *32*, 2096–2105.
- (25) Shi, H.; Zhao, Y.; Jiang, S.; Rottstegge, J.; Xin, J. H.; Wang, D.; Xu, D. *Macromolecules* **2007**, *40*, 3198–3203.
- (26) Fukuda, K.; Shibasaki, Y.; Nakahara, H. *Thin Solid Films* **1988**, *160*, 43–52.
- (27) Fujimori, A.; Shibasaki, Y.; Araki, T.; Nakahara, H. *Macromol. Chem. Phys.* **2004**, *205*, 843–854.
- (28) Caruso, F.; Furlong, D. N.; Ariga, K.; Ichinose, I.; Kunitake, T. *Langmuir* **1998**, *14*, 4559–4565.
- (29) Liao, K. L.; Du, X. Z. *J. Phys. Chem. B* **2009**, *113*, 1396–1403.
- (30) Itoh, K.; Oguri, H. *Langmuir* **2006**, *22*, 9208–9213.
- (31) Wang, J. L.; Lahav, M.; Leiserowitz, L. *Angew. Chem., Int. Ed. Engl.* **1991**, *30*, 696–698.
- (32) Hendel, R. A.; Nomura, E.; Janout, V.; Regen, S. L. *J. Am. Chem. Soc.* **1997**, *119*, 6909–6918.
- (33) Motesharei, K.; Myles, D. C. *J. Am. Chem. Soc.* **1998**, *120*, 7328–7336.
- (34) Schenning, A.P.H.J.; Peeters, E.; Meijer, E. W. *J. Am. Chem. Soc.* **2000**, *122*, 4489–4495.
- (35) Kumar, J. K.; Oliver, J. S. *J. Am. Chem. Soc.* **2002**, *124*, 11307–11314.
- (36) Puigmarti-Luis, J.; Laukhin, V.; del, Pino; Angel, Perez; Vidal-Gancedo, J.; Rovira, C.; Laukhina, E.; Amabilino, D. B. *Angew. Chem., Int. Ed.* **2007**, *46*, 238–241.
- (37) Fujimori, A.; Sato, N.; Kanai, K.; Ouchi, Y.; Seki, K. *Langmuir* **2009**, *25*, 1112–1121.
- (38) Shibasaki, Y.; Abe, Y.; Sato, N.; Fujimori, A.; Oishi, Y. *Polym. J.* **2010**, *42*, 72–80.
- (39) Fukuda, K.; Nakahara, H.; Kato, T. *J. Colloid Interface Sci.* **1976**, *54*, 430–438.
- (40) Ries, H. E., Jr.; Walker, D. C. *J. Colloid Sci.* **1961**, *16*, 361–374.
- (41) Kusanagi, H.; Tadokoro, H.; Chatani, Y. *Macromolecules* **1976**, *9*, 531–532.
- (42) Miyata, T.; Masuko, T. *Polymer* **1997**, *38*, 4003–4009.
- (43) Higashi, F.; Murakami, T. *Makromol. Chem., Rapid Commun.* **1981**, *2*, 273–277.
- (44) Takahashi, Y.; Ozaki, Y.; Takase, M.; Krigbaum, W. R. *J. Polym. Sci., B: Polym. Phys.* **1992**, *31*, 1135.
- (45) Wu, G.; Tanaka, H.; Ogata, N. *J. Polym. Sci., C: Polym. Lett.* **1981**, *19*, 343–346.
- (46) Feng, F.; Mitsuishi, M.; Miyashita, T.; Okura, I.; Asai, K.; Amao, Y. *Langmuir* **1999**, *15*, 8673–8677.
- (47) Budianto, Y.; Aoki, A.; Miyashita, T. *Macromolecules* **2003**, *36*, 8761–8765.
- (48) Endo, H.; Mitsuishi, M.; Miyashita, T. *J. Mater. Chem.* **2008**, *18*, 1302–1308.

JP909379H